The Plant Journal (2004) **38**, 725–739 doi: 10.1111/j.1365-313X.2004.02084.x

Expression profiling of *phyB* mutant demonstrates substantial contribution of other phytochromes to red-light-regulated gene expression during seedling de-etiolation

James M. Tepperman[1,2], Matthew E. Hudson[1,2,†], Rajnish Khanna[1,2], Tong Zhu[3,‡], Sherman H. Chang[3,†], Xun Wang[3,‡] and Peter H. Quail[1,2,*]

[1]*Department of Plant and Microbial Biology, University of California, Berkeley, CA 94720, USA,*
[2]*USDA/ARS-Plant Gene Expression Center, 800 Buchanan Street, Albany, CA 94710, USA, and*
[3]*Torrey Mesa Research Institute, 3115 Merryfield Row, San Diego, CA 92121, USA*

Received 27 January 2004; accepted 10 February 2004.
*For correspondence (fax +1 510 559 5678; e-mail quail@nature.berkeley.edu).
†Present address: Diversa Inc., 4995 Directors Place, San Diego, CA 92121, USA.
‡Present address: Syngenta Biotechnology, Inc., 3054 Cornwallis Road, Research Triangle Park, NC 27709, USA.

Summary

Different *Arabidopsis* phytochrome (phy) family members (phyA through phyE) display differential photosensory and/or physiological functions in regulating growth and developmental responses to light signals. To identify the genes regulated by phyB in response to continuous monochromatic red light (Rc) during the induction of seedling de-etiolation, we have performed time-course, microarray-based expression profiling of wild type (WT) and *phyB* null mutants. Comparison of the observed expression patterns with those induced by continuous monochromatic far-red light (FRc; perceived exclusively by phyA) in WT and *phyA* null-mutant seedlings suggests early convergence of the FRc and Rc photosensory pathways to control a largely common transcriptional network. *phyB* mutant seedlings retain a surprisingly high level of responsiveness to Rc for the majority of Rc-regulated genes on the microarray, indicating that one or more other phys have a major role in regulating their expression. Combined with the robust visible morphogenic phenotype of the *phyB* mutant in Rc, these data suggest that different members of the phy family act in organ-specific fashion in regulating seedling de-etiolation. Specifically, phyB appears to be the dominant, if not exclusive, photoreceptor in regulating a minority population of genes involved in suppression of hypocotyl cell elongation in response to Rc signals. By contrast, this sensory function is apparently shared by one or more other phys in regulating the majority Rc-responsive gene set involved in other important facets of the de-etiolation process in the apical region, such as cotyledon cell expansion.

Keywords: microarray, phytochromes, photosensory perception, signaling, transcriptional networks.

Introduction

The phytochrome (phy) family of photoreceptors (designated as phyA–phyE) monitor the environment for informational light signals, and induce plant growth and developmental responses appropriate to the prevailing conditions (Quail, 2002a,b; Smith, 2000). Studies with photoreceptor null mutants in *Arabidopsis* have shown that the different phy family members have differential photosensory and/or physiological functions in controlling these responses (Devlin *et al.*, 1998; Whitelam and Devlin, 1997). This is most prominent for phyA- and phyB-regulated seedling de-etiolation, where phyA is exclusively responsible for seedling responsiveness to continuous monochromatic far-red light (FRc), and phyB is considered to be predominantly responsible for responsiveness to continuous monochromatic red light (Rc; Fankhauser and Chory, 1997; Neff *et al.*, 2000; Quail, 1998; Quail *et al.*, 1995; Whitelam and Devlin, 1997; Whitelam *et al.*, 1998).

Previously, to identify the genes specifically regulated by phyA in driving the de-etiolation process, we performed expression profile analysis of *Arabidopsis* wild type (WT)

and *phyA* null mutants in response to FRc, using Affymetrix high-density oligonucleotide microarrays (Tepperman *et al.*, 2001). The data showed that 10% of the genes represented on the array are regulated by phyA in response to the light signal. Robust, temporally co-ordinate regulation was observed for all functional categories of genes over the 24-h time-course examined, consistent with the major redirection of development in the transition from heterotrophic to autotrophic growth. Most significantly, however, 44% of the small group of functionally classified genes, responding to the signal within 1 h, are predicted to encode multiple classes of transcriptional regulators. Because several of these factors already had established or putative roles in controlling one or other major facets of photomorphogenesis, the data suggest that they may represent a master set of transcriptional regulators that orchestrate the expression of the downstream target genes that elaborate this process. Similarly, the rapid responsiveness of these genes suggests that they may be direct targets of phyA signaling. Thus, these data have provided initial insight into the transcriptional networks, linking phyA photoperception to a major developmental transition (Quail, 2002a,b; Tepperman *et al.*, 2001).

To begin to understand the differential photosensory activities of phyA and phyB in regulating this same developmental response, it is necessary to define the genes regulated in common by both photoreceptor pathways, and those which may exhibit specificity to one or the other pathway. To this end, here, we examine the gene expression profiles of WT and *phyB* mutant *Arabidopsis* seedlings in response to Rc over a 24-h time-course, using Affymetrix oligonucleotide microarrays and the same basic experimental design as used previously for phyA (Tepperman *et al.*, 2001).

Results and discussion

Do red and far-red wavelengths regulate the same genes in WT seedlings?

The well-established contrasting visible phenotypes of *phyA* and *phyB* null-mutant seedlings in response to the Rc and FRc conditions used here are shown in Figure S1 (von Arnim and Deng, 1996; Fankhauser, 2001; Fankhauser and Chory, 1997; Neff *et al.*, 2000; Quail, 2002a,b; Whitelam and Devlin, 1997; Whitelam *et al.*, 1998).

To provide a basic, photobiological framework for comparing phyA and phyB activities, we initially compared the expression of the genes induced or repressed by FRc in WT seedlings in our previous experiment (Tepperman *et al.*, 2001) with those responding to Rc in WT seedlings in the present experiment. To facilitate this comparison, we first re-analyzed the data from the original FRc experiment, using an improved algorithm (MAS 5.0) from Affymetrix (Affymetrix, 2001; Hubbell *et al.*, 2002; Liu *et al.*, 2002; see Note S1 for details). This analysis resulted in 858 genes being classified as FRc-regulated (Figure 1; see Tables S1–S10 for gene list and data).

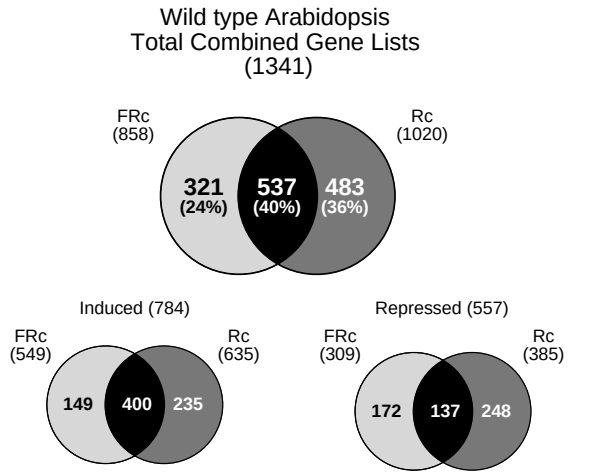

Figure 1. Numbers of genes defined as responding to FRc and/or Rc in WT *Arabidopsis* seedlings.
Venn diagrams show the number of genes classified as responding to either FRc only (left), Rc only (right), or both FRc and Rc (center). Top: total number of responding genes. Bottom: numbers of responsive genes induced or repressed by each wavelength. The total number of genes in each category is shown in parentheses.

Analysis of the expression profiles of Rc-irradiated WT seedlings in the present study identified a total of 1020 genes as being Rc-responsive (Figure 1), corresponding to about 13% of the genes represented on the microarray. These genes are listed in Tables S11–S13. Of these, 62% were induced and 38% were repressed, with 14% exhibiting changes in transcript abundance within 1 h of exposure to Rc (early-response genes) and the remaining 86% first displaying changes at a later time during the remainder of the 24-h irradiation period (late-response genes; Table 1). A list of all Rc-responsive genes, assigned to each functional category, can be found in Tables S11–S13.

Initial comparison of the FRc- and Rc-responsive gene lists suggested only limited overlap between the two (40%), with 24 and 36% being FRc- and Rc-specific, respectively (Figure 1). However, because of the low stringency of the primary qualifying criteria, this apparent dichotomy in wavelength responsiveness is potentially misleading (see Note S2 for more detailed discussion). We, therefore, developed a more robust index of light responsiveness for a more quantitative evaluation and comparison of responsiveness to the two wavelengths. This index, termed mean fold induction (MFI) for upregulated genes, or mean fold repression (MFR) for downregulated genes, is determined separately for the FRc- and Rc-treated WT seedlings for each gene, and the ratio of these two values is termed

Table 1 Number of Rc-regulated genes categorized by functional class and temporal expression pattern

	Early-response genes (1 h)		Late-response genes (3–24 h)		
Functional classification	Induced	Repressed	Induced	Repressed	Total
Transcription (Tx)	21	4	21	45	91
Photosynthesis/chloroplast (P/C)	10	1	105	3	119
Cellular metabolism (CM)	12	2	112	77	203
Signaling (S)	7	1	28	27	63
Transporters (Tr)	8	0	21	11	40
Growth and development (G/D)	3	2	12	16	33
Hormone-pathway related (H)	3	4	9	18	34
Stress/defense (S/D)	21	1	43	27	92
Hypothetical/unknown (H/U)	29	9	170	137	345
Total	114	24	521	361	1020

Genes represented on the microarray, whose mRNA abundance was either increased (induced) or decreased (repressed) twofold or more under red light within 1 h (early), or between 3 and 24 h (late) of the start of Rc irradiation, were scored and classified into the broad functional categories shown, according to established or putative function in the plant.

the mean fold induction ratio (MFIR) or mean fold repression ratio (MFRR; see Experimental procedures).

The MFIR and MFRR values were calculated for all 1341 genes on the combined FRc and Rc gene lists (MFIR for the 784 induced genes, MFRR for the 557 repressed genes; see Figure 1), and the genes within each set were arrayed in a continuum in rank order of descending MFIR (Figure 2a) or MFRR (Figure 3a) value. The combined list of all FRc- and Rc-responsive genes is presented in Table S14. The curves depicting the distribution of these values for both the FRc/Rc ratio and its reciprocal Rc/FRc ratio are included in Figures 2(a) and 3(a). The genes in these arrays were divided into seven bins (A–G) based on MFIR or MFRR value, and the number of genes in each bin is shown in histogram format in the inset. The statistical reliability of the differences in the two MFI or MFR values used to calculate the MFIR or MFRR value for each gene was also assessed using a paired *t*-test (see Experimental proce-

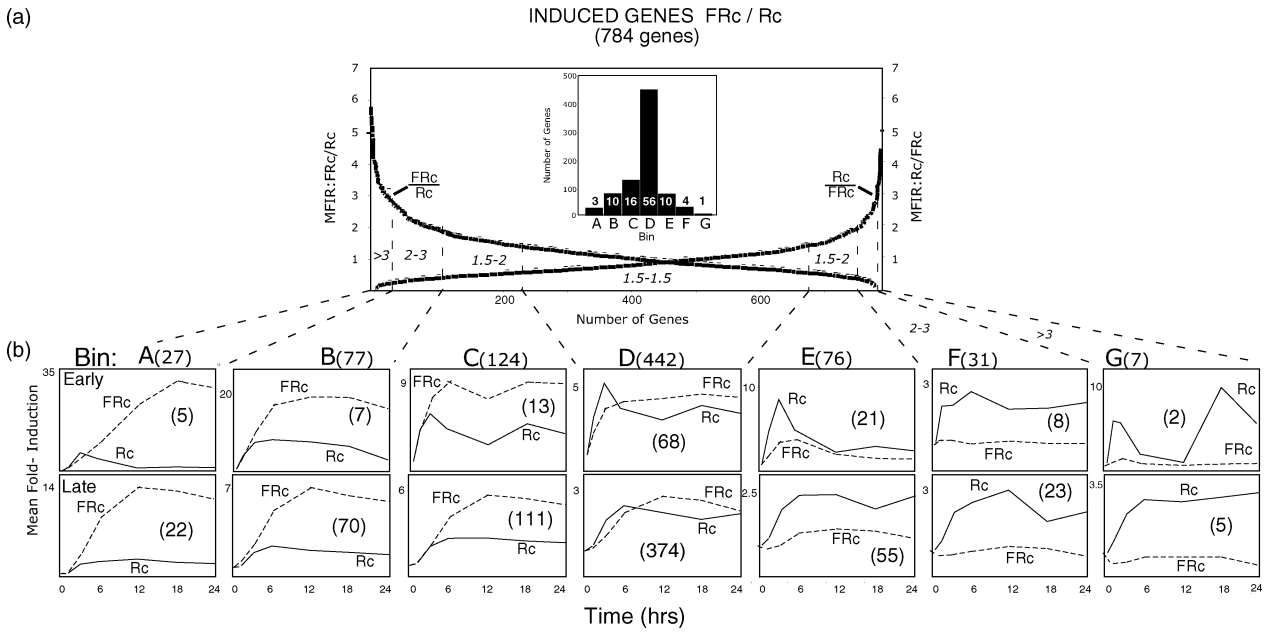

Figure 2. Induced genes arrayed in rank order of relative responsiveness to FRc or Rc in WT *Arabidopsis* seedlings.
(a) Curves depicting distribution of all induced genes on the combined list (784) in order of descending MFIR for FRc/Rc (MFIR: FRc/Rc), and the reciprocal MFIR for Rc/FRc (MFIR: Rc/FRc). Vertical dashed lines divide the array into bins (A–G) according to MFIR value. Inset: histogram showing the total number of genes in each bin. Internal values show percentage distribution between bins.
(b) Mean 24-h time-course curves for all early-response (top) and late-response (bottom) genes in each bin in FRc or Rc. Data are plotted as fold-induction relative to the level of expression in WT, dark-control seedlings at time zero of the 24-h irradiation period. Note that fold-induction scale varies between panels. Numbers in parentheses represent the total number of genes in each bin or panel indicated.

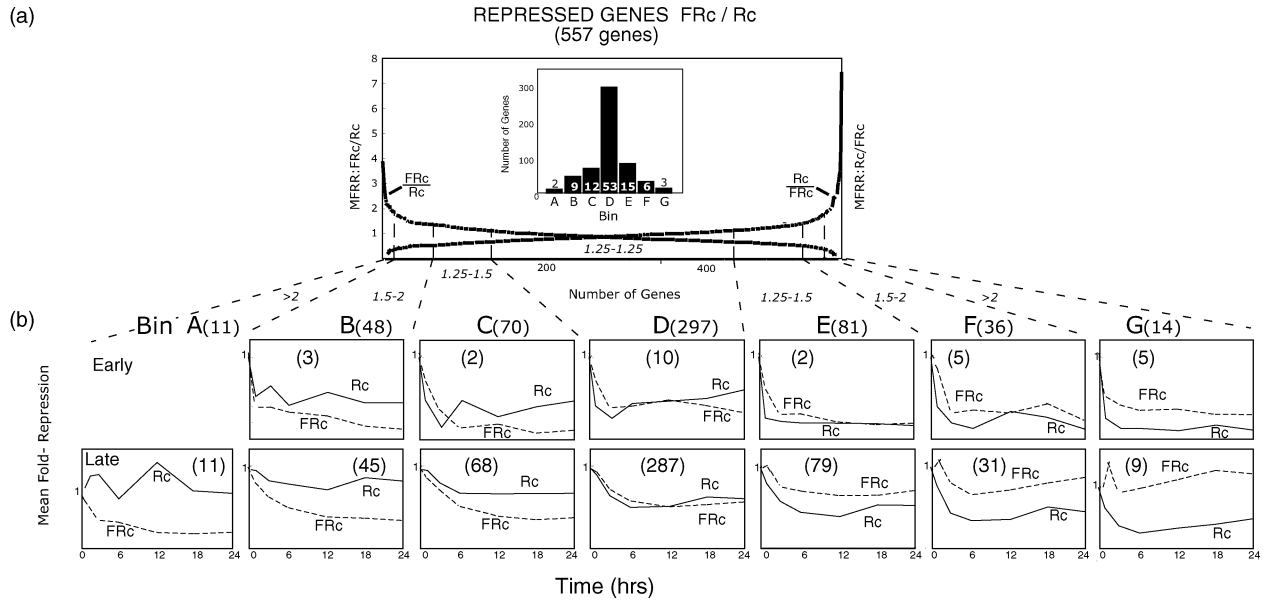

Figure 3. Repressed genes arrayed in rank order of relative responsiveness to FRc or Rc in WT *Arabidopsis* seedlings.
(a) Curves depicting distribution of all repressed genes on the combined list (557) in order of descending MFRR for FRc/Rc (MFRR: FRc/Rc), and the reciprocal MFRR for Rc/FRc (MFRR: Rc/FRc). Vertical dashed lines divide the array into bins (A–G) according to MFRR value. Inset: histogram showing the total number of genes in each bin. Internal values show percentage distribution between bins.
(b) Mean 24-h time-course curves for all early-response (top) and late-response (bottom) genes in each bin in FRc or Rc. Data are plotted as fold-repression relative to the level of expression in WT, dark-control seedlings at time zero of the 24-h irradiation period. Note that fold-repression scale varies between panels. Numbers in parentheses represent the total number of genes in each bin or panel indicated.

dures). The *P*-values for each gene from this test are included in Table S14, and are plotted against the corresponding MFIR or MFRR values in Figures S2 and S3, respectively. The percentage of genes in each MFIR or MFRR bin of Figures 2 and 3 with *P*-values of $\leq$0.05 are also plotted in these figures. Such *P*-values indicate that the mean expression values used to calculate the corresponding MFIR/MFRR values for these genes have a high probability of also being statistically different from each other in the outside bins A and G of Figures 2 and 3, declining to a minimum in the central bin D (Figures S2 and S3). While it is difficult to determine from these data which, if any, of these genes exhibit biologically meaningful differences in responsiveness to FRc and Rc, clearly those in the central region of these distributions are least likely, whereas those at the extremes are most likely to represent such differences (Figures 2 and 3).

Overall, these data indicate that about 82% of the light-responsive genes respond more or less equivalently to both Rc and FRc, another 14% respond to both wavelengths, but exhibit partially greater responsiveness to one or the other, and the remaining approximately 4% respond relatively more robustly to either FRc or Rc (see Note S3 for details). It should be noted, however, that very few genes displayed a robust responsiveness to one wavelength coupled with an apparent complete absence of responsiveness to the other wavelength. On the contrary, the vast majority of genes exhibit responsiveness to both FRc and Rc wavelengths to one extent or another. The 10 genes most closely approaching such robust qualitative differences in wavelength responsiveness are listed in Table 2.

The mean time-course curves for all early- and late-response genes in each bin are depicted in Figures 2(b) and 3(b). These data show the progression from dominant FRc responsiveness in bin A on the left, through approximately equivalent FRc- and Rc responsiveness in bin D in the center, to dominant Rc responsiveness in bin G on the right. The difference in temporal response pattern between early and late genes is evident, but the time-course profiles in FRc and Rc are, in general, similar, suggesting temporal co-ordinate regulation of expression by the two wavelengths. Individual curves for each gene, as well as histograms for the 1-h data points used to define early-response genes, are accessible from the gene lists in Tables S14–S20.

The distribution of the genes in different functional categories among the wavelength-responsiveness bins and temporal-response categories are depicted in Figures S4 and S5. The designated functional categories for all genes on the combined list are contained in Tables S14–S20. Overall, the distribution of genes among different functional categories in each wavelength-responsiveness bin does not indicate any marked, systematic, preferential induction or repression of any broad group of genes by FRc or Rc. Thus, no markedly preferential regulation of any

Table 2 Genes displaying apparent qualitatively robust differences in responsiveness to FRc and Rc

Response direction	Temporal response category	Bin A[a] (FRc > Rc)			Bin G[a] (Rc > FRc)		
		Gene name	AGI number	*P*-value[b]	Gene name	AGI number	*P*-value[b]
Induced	Early	*bHLH-T16*	At4g00050	0.011	*LHY*	At1g01060	0.040
	Late	Methionine sulfoxide reductase A	At4g04840	0.015	*AQUAPORIN*	At2g16850	0.006
		ENDOXYLOGLUCAN TRANSFERASE	At5g65730	0.039	*HSP83*	At5g52640	0.011
		Heat shock	At2g04030	0.004	–	–	–
Repressed	Early	None	–	–	*bHLH-T61*	At2g46970	0.002
		–	–	–	*HAT4*	At4g16780	0.003
	Late	β-Expansin	At2g20750	0.005	None	–	–

[a]Bin designation from Figures 2 and 3.
[b]*P*-values indicate statistical significance of the difference in mean expression levels between FRc and Rc treatments as determined by *t*-test analysis of time-course data.

particular cellular process by either wavelength is apparent. On the other hand, it is notable that the four early-response, putative transcriptional regulators, bHLH (basic helix-loop-helix)-T16 (also called AtbHLH16), LHY (late elongated hypocotyl), HAT (homeobox *Arabidopsis thaliana*)4, and bHLH-T61 (also called AtbHLH124 and PIL (Pif3-like)1; Heim *et al.*, 2003; Toledo-Ortiz *et al.*, 2003; Yamashino *et al.*, 2003), do display relatively robust and statistically significant selective responsiveness to either FRc (bHLH-T16) or Rc (LHY, HAT4, and bHLH-T61), respectively. The individual response curves for these genes are shown in Figure S6.

By contrast, the vast majority of early-response genes encoding potential regulatory factors, such as transcription factors and signaling components, are in the central bins C–E (Figures S4 and S5), reflecting comparable responsiveness to both wavelengths. In fact, transcription-factor genes are the single most abundant class of functionally classifiable, inducible, early-response genes in bin D, where both wavelengths are about equally effective (Figure S4). Strikingly, all except two of the transcription-factor genes, previously identified as responding rapidly to FRc (Tepperman *et al.*, 2001), are also early-response genes in Rc. Individual response curves for some of these genes are shown in Figure S7.

These data suggest that the core set of transcription-factor genes, initially identified as possible direct targets of phyA signaling, are also targets of Rc signaling. Because this original set of genes comprises 70% of the total number of early-response, transcription-factor genes responding to both wavelengths, it would appear that this set is indeed likely to encode a master set of transcriptional regulators centrally involved in orchestrating the expression of a common array of downstream genes in response to both Rc and FRc wavelengths.

It is noteworthy that all the early-response, signaling-component genes, originally identified as FRc-responsive (Tepperman *et al.*, 2001), are also Rc-responsive, and are categorized in bins D and E of Figures 2 and 3, consistent with the involvement in a common pathway. Similarly, several genes involved in hormone-regulated growth responses, including the auxin-related genes *GH3*, *IAA19*, *IAA* (indole acetic acid regulated)*20*, and *SAUR-AC* (small auxin up RNA), and the ethylene-related gene *HOOKLESS*, all exhibit rapid responsiveness to the light signals. These data are perhaps consistent with a role of these genes in mediating early steps in the FRc- and Rc-induced changes in hypocotyl and cotyledon cell expansion rates, including hook opening.

More detailed consideration of the distribution of functionally classifiable genes across the wavelength-responsiveness bins and temporal-response categories is available in Note S4. In addition, example curves of some late-response genes, displaying robust and statistically significant differences in wavelength responsiveness, are shown in Figure S8.

Is phyB the predominant photoreceptor for Rc-regulated gene expression during de-etiolation?

Previously, the genes we identified as being phyA-regulated in response to FRc exhibited, on average, robust differences in expression between the WT and the *phyA* null mutant (Tepperman *et al.*, 2001). This contrast in responsiveness is summarized in Figure S9(a,b) for the phyA-regulated gene list, resulting from the present re-analysis of the previous FRc experiment. This figure shows the mean time-course for induced and repressed genes in WT and *phyA* mutant. Whereas these genes clearly respond to the FRc signal in the WT, there is essentially no detectable response in the null mutant, consistent with the exclusive role of phyA mediating the FRc signal in regulating this gene set.

Initially surprising for us, given the prevailing view of the dominant role of phyB in Rc-induced de-etiolation (Fankhauser, 2001; Neff *et al.*, 2000; Quail, 2002a,b; Whitelam and Devlin, 1997), similar mean curves computed for the Rc-regulated gene set identified here resulted in markedly smaller average differences between the WT and

phyB null mutant (Figure S9c,d). In contrast to the *phyA* mutant, the *phyB* mutant retains substantial responsiveness to the Rc signal. To determine the basis for this pattern, we performed an analysis of WT and *phyB* expression profiles similar to that described above in Figures 2 and 3. In this case, we computed the MFI (or MFR) values for each gene in WT and *phyB* mutant seedlings, separately, in response to Rc, and determined the ratio of these two values (i.e. [MFI (or MFR) for WT]/[MFI (or MFR) for *phyB*]) for each gene. This ratio was designated as MFIR (or MFRR) as before. The genes within the induced and repressed sets were then arrayed in a continuum in rank order of descending MFIR (Figure 4) or MFRR (Figure 5) value, respectively. The curves depicting the distribution of these values are shown in Figures 4(a) and 5(a). The genes in these arrays were divided into five bins (A–E), based on MFIR or MFRR value, and the number of genes in each bin is shown in histogram format in the inset.

The data show that there is a continuous gradation in relative responsiveness of WT and *phyB* seedlings to Rc, ranging from no apparent difference for some genes to relatively robust average differences for others (Figures 4a and 5a). Of the induced genes, 60% exhibit less than a 1.25-fold difference between WT and mutant in average responsiveness to Rc (Figure 4a, bins D and E), and another 24% less than a 1.5-fold difference (Figure 4a, bin C). This result indicates that the majority in this set (84%) are either not regulated by phyB, or only marginally so, in response to Rc. On the other hand, 11% of these genes exhibit a 1.5- to 2-fold greater induction in WT than in the *phyB* mutant (Figure 4a, bin B), and 5% a more than 2-fold greater induction (Figure 4a, bin A), consistent with a more significant role of phyB in regulating this subset of genes. Similarly, of the repressed genes, 68% exhibit less than a 1.25-fold difference between WT and mutant in average responsiveness to Rc (Figure 5a, bins D and E), and another 23% less than a 1.5-fold difference (Figure 5a, bin C), suggesting that the majority in this set (91%) are either not regulated by phyB, or only marginally so. On the other hand, 9% of these genes displayed a 1.5- to 2-fold greater

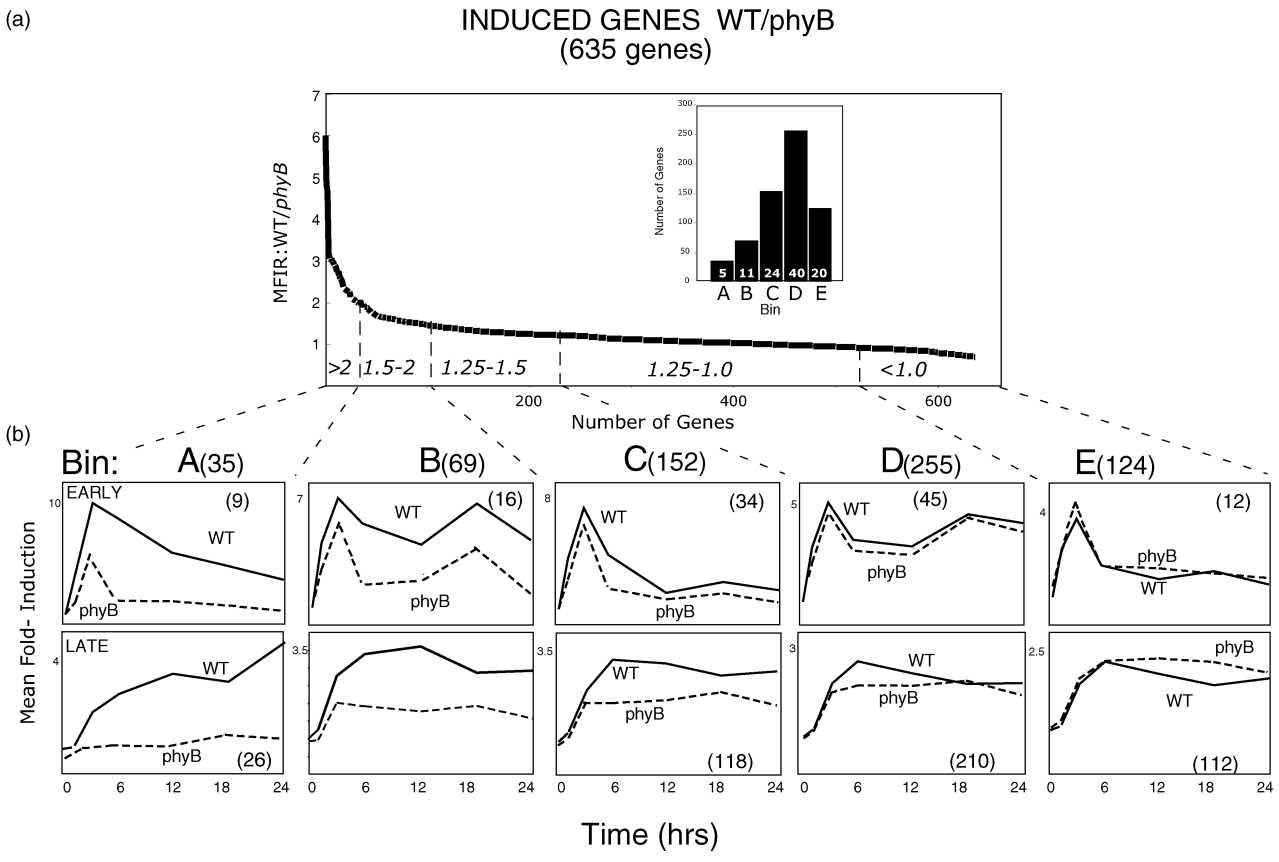

Figure 4. Induced genes arrayed in rank order of relative responsiveness to Rc in WT compared to *phyB* Arabidopsis seedlings.
(a) Curve depicting distribution of all Rc-induced genes on the list (635) in order of descending MFIR for WT/*phyB* (MFIR: WT/*phyB*). Vertical dashed lines divide the array into bins (A–E) according to MFIR value. Inset: histogram showing the total number of genes in each bin. Internal values show percentage distribution between bins.
(b) Mean 24-h time-course curves for all early-response (top) and late-response (bottom) genes in each bin in WT and *phyB*. Data are plotted as fold-induction relative to the level of expression in WT, dark-control seedlings at time zero of the 24-h irradiation period. Note that fold-induction scale varies between panels. Numbers in parentheses represent the total number of genes in each bin or panel indicated.

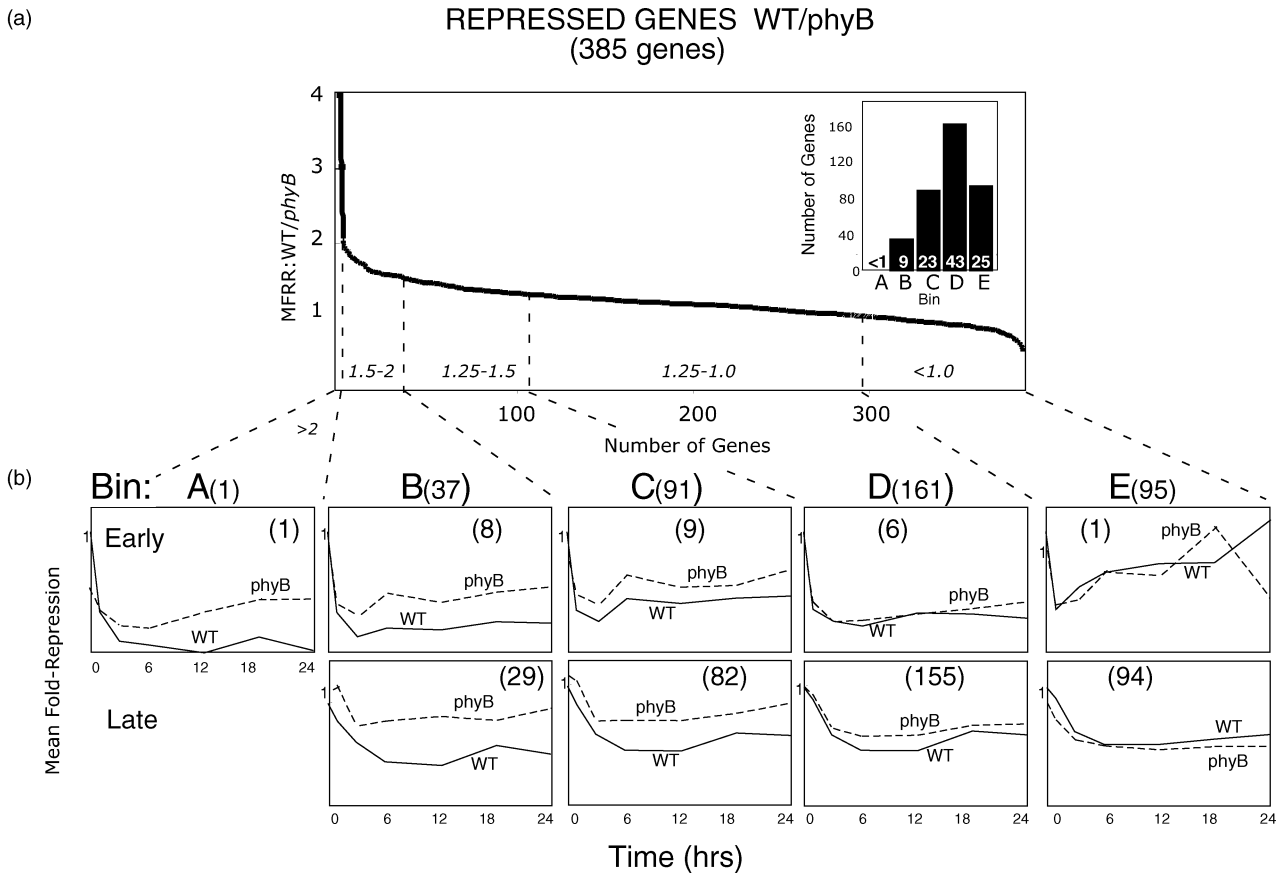

Figure 5. Repressed genes arrayed in rank order of relative responsiveness to Rc in WT compared to *phyB Arabidopsis* seedlings.
(a) Curve depicting distribution of all Rc-repressed genes on the list (385) in order of descending MFRR for WT/*phyB* (MFRR: WT/*phyB*). Vertical dashed lines divide the array into bins (A–E) according to MFRR value. Inset: histogram showing the total number of genes in each bin. Internal values show percentage distribution between bins.
(b) Mean 24-h time-course curves for all early-response (top) and late-response (bottom) genes in each bin in WT and *phyB*. Data are plotted as fold-repression relative to the level of expression in WT, dark-control seedlings at time zero of the 24-h irradiation period. Note that fold-repression scale varies between panels. Numbers in parentheses represent the total number of genes in each bin or panel indicated.

repression in WT than in mutant (Figure 5a, bin B), and 0.2% a more than twofold greater repression (Figure 5a, bin A).

A paired *t*-test was used to assess the statistical significance of the differences in the two MFI or MFR values used to calculate the MFIR or MFRR for each gene in Figures 4 and 5, and the *P*-values obtained are tabulated in Table S14. These *P*-values are plotted against the corresponding MFIR or MFRR values in Figures S10 and S11, and the percentage of genes in each MFIR or MFRR bin of Figures 4 and 5 having *P*-values of $\leq$0.05 are also plotted in these figures. The data show that there is a strong correlation between the robustness of the difference in WT and *phyB* gene expression, defined by the MFIR/MFRR index and the statistical significance of this difference. High MFIR and MFRR values are generally correlated with low *P*-values and vice versa.

Collectively, these induction and repression data suggest that, overall, about 62% of Rc-responsive genes exhibit little, if any, detectable dependence on phyB for regulation, about 24% exhibit marginal dependence, and the remaining 14% exhibit significant to relatively robust dependence on phyB for responsiveness to Rc. Significantly, however, we detected very few genes in our analysis that displayed no apparent responsiveness to Rc in the *phyB* mutant. The few genes that most closely approach this latter behavior are listed in Table 3, and some representative individual curves are shown in Figures S12 and S13 (right-hand panels). In addition, some representative individual curves for genes showing little or no apparent difference between WT and *phyB* in responsiveness to Rc are shown in Figure S14 (right-hand panels). The corresponding curves for WT and *phyA* in FRc are included for comparison in each case (Figures S12–S14, left-hand panels). These results suggest that one or more other members of the phy family (phyA, phyC, phyD, and/or phyE) play a dominant role in regulating the majority of Rc-responsive genes (86%), rather than phyB, and that despite phyB dominance in regulating some of the remaining minority of Rc-responsive genes, other phys appear to contribute partial residual activity.

Table 3 Genes displaying relatively robust differences in responsiveness to Rc between WT and *phyB* mutant[a]

Temporal response category	Response direction					
	Induced			Repressed		
	Gene name	AGI number	*P*-value[b]	Gene name	AGI number	*P*-value[b]
Early	*AIP*	At4g38840	0.013	*bHLH T61*	At2g46970	0.005
	GI	At1g22770	0.001	*PORA*	At5g54190	0.0006
	β-Amylase	At4g17090	0.008	*SAUR-AC*-like	At4g13790	0.005
	CELLULOSE SYNTHASE ISOLOG	At4g23990	0.012	*HOOKLESS*	At4g37580	0.018
	EP1-L	At1g78820	0.0006	–	–	–
Late	*phyD*	At4g16250	0.029	*ARF-L*	At4g30080	0.003
	Endotransglucosylase	At4g37800	0.037	–	–	–
	AQUAPORIN	At2g16850	0.002	–	–	–
	Putative auxin-regulated	At2g21210	0.019	–	–	–
	GAST1/GA-regulated	At1g22690	0.035	–	–	–
	Unknown	At2g21860	0.001	–	–	–
	ACC OXIDASE	At1g05010	0.017	–	–	–

[a]From bin A (Figures 4 and 5).
[b]*P*-values indicate statistical significance of the difference in mean expression levels between WT and *phyB* in Rc as determined by *t*-test analysis of time-course data.

Differential photosensory and regulatory activity among phy family members

The above conclusion is summarized schematically and expanded to include the phyA data in Figure 6. This analysis was accomplished by merging the classification of the gene lists determined in the FRc/Rc comparison in Figures 2 and 3, with that of the WT/*phyB* comparison in Figures 4 and 5. For simplicity, genes in bins A–E in Figures 2 and 3 were classified as phyA-regulated, and those in bins F and G as non-phyA-regulated. The Rc-regulated genes in bins A and B of Figures 4 and 5 were classified as phyB-regulated, and those in bins C–E as non-phyB-regulated. It should be emphasized, however, that because these designations are not absolute, individual genes within each broad class may not comply rigorously with the nominal classification. For example, a number of genes in bins F and G of Figure 2, which are classified as 'non-phyA-regulated' based on their presence in these bins, do indeed exhibit significant FRc responsiveness. These genes are in these bins because the Rc responsiveness is markedly greater than that of FRc, resulting in detection of a robust differential in responsiveness to the two wavelengths (quantified as MFIR or MFRR). This is most striking for the transcription-factor genes, *LHY*, *HAT4*, and *bHLH-T61*, which were shown previously to be phyA-regulated, but, as shown here, exhibit much stronger Rc than FRc responsiveness (Figure S6).

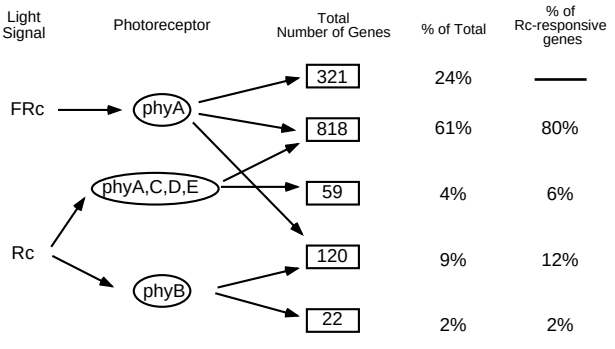

Figure 6. Channeling of photosensory information.
Simplified schematic summary depicting the channeling of photosensory information by the phy family to photoresponsive gene sets involved in seedling de-etiolation.

Applying these criteria to the combined gene lists (1341 genes) resulted in five categories of genes based on the predominant wavelength and photoreceptor regulating expression (Figure 6). This scheme shows the extensive overlap in genes regulated by both FRc and Rc wavelengths, and the dichotomy within the Rc-regulated genes between those regulated to a significant extent by phyB and those regulated predominantly by one or more other family members (phyA, phyC, phyD, or phyE). Moreover, it shows the further dichotomy within each Rc-regulated subset between genes that are also phyA-regulated in FRc, and those which are not. The curves shown in Figures S12–S14 (right-hand panels) for the individual genes, representing some of these Rc-regulated subsets, are compared with the corresponding curves for the WT and *phyA* mutants in FRc (left-hand panels). These data reinforce the generality that most genes are regulated in parallel by both wavelengths, and illustrate the point that genes, robustly regulated by phyA in FRc, range from relatively robust to undetectable dependence on phyB for Rc responsiveness.

To identify genes most likely to be involved in primary, light-responsive events controlled predominantly by phyB, we further classified the Rc-regulated genes in each bin

both into early and late temporal-response categories (Figures 4b and 5b), and functional categories (Figures S15b and S16b). Total number of genes in each category are shown in Table 1, and the designated categories for each individual gene are contained in Tables S11–S13 and S21–S27. The mean time-course curves for all genes in each bin are depicted in Figures 4(b) and 5(b), showing the progression from relatively robust differential responsiveness of WT and *phyB* seedlings in bin A on the left, to approximately equivalent responsiveness in bins D and E on the right. The difference in temporal response patterns of early- and late-response genes is also evident, as is the tendency for early-response genes to exhibit an acute transient induction, compared to the late-response genes, which display a more sustained response. Individual curves for each gene, as well as histograms for the 1-h data points used to define the early-response genes, are accessible from the gene lists in Tables S11–S13 and S21–S27. Representative individual curves for some early-response and late-response genes are shown in Figure S12, and Figures S13 and S14, respectively.

Of the induced genes most robustly dependent on phyB for Rc responsiveness (Figure 4, bin A), genes for two potential signaling components, extracellular protein (EP)1 (AAC83044) and gigantea (GI) (CAB56039), exhibit early responsiveness, but no transcription-factor genes are represented. Of the induced genes moderately dependent on phyB for Rc responsiveness (Figure 4, bin B), six putative transcription-factor genes, *CBF* (CRT/DRE binding factor)*2* (encoding AAD15976), *ZF* (zinc finger)*3* (encoding AAD26481), *MYB* (myeloblastic)*106* (encoding AAF26160), *ZF6* (encoding AAD23680), *RAP* (RNA polymerase associated protein)*2.6* (encoding AAC36019), and *ZF7* (encoding AAB80422), and one signaling component gene, *SPA* (suppressor of phytochrome A)*1* (encoding AAD30124), exhibit early responsiveness. Of these transcription-factor genes, the first five are also robustly phyA-dependent in FRc, as are the two signaling components *EP1* and *SPA1*. The remaining 15 Rc-responsive, early-induced, transcription-factor genes exhibit very marginal to no apparent dependency on phyB. Eleven (73%) of these 15 genes are robustly phyA-dependent in FRc, with the remaining four (27%) being newly identified, preferentially Rc-responsive genes. Of the repressed genes, four transcription-factor genes, *HAT4* (encoding CAA79670), *GATA* (encoding AAD3283), *ATHB* (*A. thaliana* homeobox)*4* (encoding AAC31833), and *bHLH-T61* (encoding AAC34226), exhibit early responsiveness. All four of these genes respond robustly to both FRc and Rc in WT seedlings. *bHLH-T61* and *ATHB4* display moderate dependence on phyB for Rc responsiveness, whereas *HAT4* and *GATA* exhibit marginal or no apparent phyB dependence. These data are summarized schematically in Figure 7 (left-hand column), and the time-course curves for each transcription-factor gene, with the corresponding *P*-value for statistical confidence of differential expression in WT and *phyB*, are shown in Figure S17.

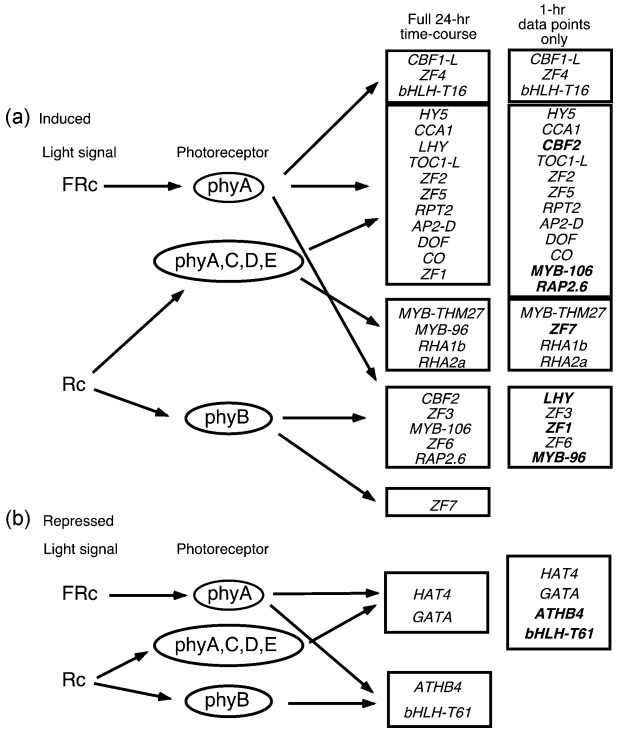

Figure 7. Photosensory information channeling to early-response transcription factor genes.
Simplified schematic summary depicting the channeling of photosensory information by the phy family to various subsets of early-response, transcription-factor genes that are either (a) induced or (b) repressed in response to FRc and/or Rc signals during seedling de-etiolation. Left column: classification based on analysis of expression data over the full 24-h time-course for each gene. Right column: classification based on analysis of expression levels at the 1-h data point only. Genes that change category as a result of the 1-h compared to the 24-h analysis are shown in bold-face type. AGI numbers and encoded protein accession numbers (in parentheses) for designated genes: *CBF1-L*: At4g25480 (CAA18178); *ZF4*: At4g38960 (CAB38816); *bHLH-T16*: AT4g00050 (AAC19308); *HY5*: At5g11260 (BAA21327); *CCA1*: At2g46830 (AAC33507); *LHY*: At1g01060 (CAB42406); *TOC1-L*: At2g46790 (AAC33497); *ZF2*: At1g06040 (CAA64819); *ZF5*: At5g59820 (CAA67232); *RPT2*: At2g30520 (AAB63085); *AP2-D*: At2g28550 (AAD21489); *DOF*: At3g47500 (AAC28390); *CO*: At5g15850 (CAA71588); *ZF1*: At3g02830 (AAD33769); *MYB-THM27*: At1g22640 (AAC25522); *MYB-96*: At5g62470 (CAA09728); *RHA1b*: At4g11360 (AAC68670); *RHA2a*: At1g15100 (AAD39638); *CBF2*: At4g25470 (AAD15976); *ZF3*: At2g31380 (AAD26481); *MYB-106*: At5g15310 (AAF26160); *ZF6*: At2g21320 (AAD23680); *RAP2.6*: At1g43160 (AAC36019); *ZF7*: At5g04340 (AAB80922); *HAT4*: At4g16780 (CAA79670); *GATA*: At2g45050 (AAD32831); *ATHB4*: At2g44910 (AAC31833); *bHLH-T61*: At2g46970 (AAC34226).

Taken together, the data show that although the majority of early-response, transcription-factor genes shown here, and previously (Tepperman *et al.*, 2001), to be robustly phyA-dependent in responsiveness to FRc are also strongly Rc-light-responsive (87%), only 30% of these exhibit apparent phyB-dependency for the Rc response. This result indicates

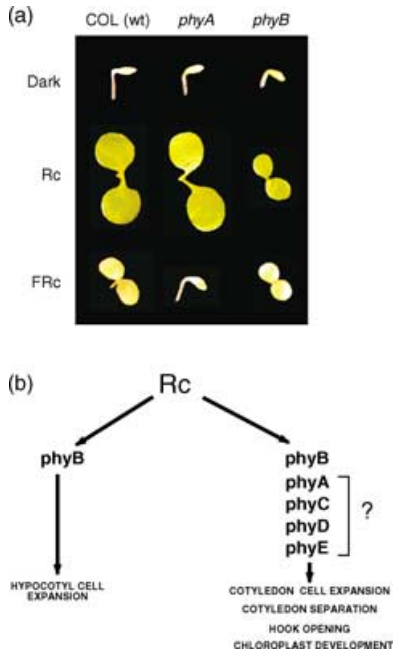

Figure 8. Multiple phys mediate Rc-induced seedling de-etiolation in a partially organ-specific manner.
(a) Seedling apical-zone photomorphogenic phenotypes in *phyA* and *phyB* null-mutant seedlings in response to Rc or FRc. Growth conditions as in Figure S1.
(b) Schematic indicating organ-specific differences in signaling activity among phy family members in response to Rc. It is proposed that phyB dominates in regulating hypocotyl cell elongation in response to Rc, but that one or more other family members (phyA, phyC, phyD, and/or phyE; uncertainty indicated by query), in addition to phyB, are involved in regulating various aspects of apical-zone responsiveness to Rc, including hook opening, cotyledon separation and expansion, and chloroplast development.

that phy family members, other than phyB (i.e. phyA, phyC, phyD, and/or phyE),mediate the Rc signal in regulating the majority of these genes (Figure 7, left-hand column). Similarly, of the five transcription-factor genes newly identified here as being Rc- but not FRc-responsive, only one, *ZF7* (encoding AAB80422), exhibits relatively robust phyB-dependency by these criteria. The remainder, *MYB-THM* (tomato hypocotyl MYB)*27* (encoding AAC25522), *MYB96* (encoding CAA09728), *RHA* (ringfinger H2A)*1b* (encoding AAC68670), and *RHA2a* (encoding AAD39638), appear to be regulated by other phy family members in response to Rc (Figure 7, left-hand column).

Based on the premise that the genes most likely to be primary targets of phyB signaling will be those that not only respond rapidly to Rc, but in addition display rapid differences in responsiveness between WT and *phyB* to Rc, we further analyzed the early-response genes for the extent of phyB contribution to the Rc response at 1 h only (Figure 7, right-hand column; see Note S5 and Figures S18–S20 for details). Collectively, this analysis suggests that five transcription-factor genes, *LHY*, *ZF3*, *ZF1*, *ZF6*, and *MYB-96*, are potential primary targets of phyB signaling, albeit only transiently for *LHY*, *ZF1*, and *MYB-96*. The other genes exhibiting significant phyB-dependence, *CBF2*, *MYB-106*, *RAP2.6*, *ZF7*, *ATHB4*, and *bHLH-T61*, do so later in the time-course, and may therefore be more indirect targets of the phyB pathway.

The general pattern of photoresponse categories for the transcription-factor genes depicted in Figure 7 parallels that for the overall light-regulated gene population (Figure 6). It is possible, therefore, that the segregation of the transcription-factor genes into these response categories (Figure 7) may represent the initial segmentation of the transcriptional network into the major branches that regulate the downstream genes in the corresponding response categories observed in the overall gene population (Figure 6). The data suggest that the global patterns of gene expression observed after long-term irradiations (5–7 days) with Rc or FRc (Ma *et al.*, 2001) may have been established within the initial 12-h transition period following first exposure to light, as defined here.

Can the absence of a robust molecular phenotype in the phyB *mutant in Rc be reconciled with the presence of an apparently robust visible phenotype?*

The apparent discrepancy between the strengths of the gene-expression (molecular; Figures S9 and 6) and morphological (Figure S1) phenotypes in Rc that result from the absence of phyB may be resolvable by considering different facets of the seedling de-etiolation response separately. Specifically, closer inspection of the *phyB* mutant seedlings grown in Rc indicates that whereas hypocotyl elongation is essentially unresponsive to the Rc signal, the tissues in the apical zone of the seedling do indeed respond, at least partially: the apical hook unfolds, and the cotyledons separate and partially expand (Figures S1 and 8a). This behavior is in striking contrast to that of the *phyA* mutant in FRc, where, in addition to the hypocotyl being unresponsive, the apical-zone tissues are also completely insensitive to the light signal (Figures S1 and 8a). This observation suggests that phyB certainly is the dominant photoreceptor for Rc-imposed suppression of hypocotyl cell elongation, but that, while it is partially responsible for regulating cotyledon cell expansion, one or more other members of the family (phyA, phyC, phyD, and/or phyE) are also active in hook unbending, and cotyledon separation and expansion in response to Rc (Figure 8b). Similar observations have been reported by previous authors (Franklin *et al.*, 2003; Reed *et al.*, 1993, 1994; Whitelam *et al.*, 1998).

Because RNA was extracted from whole seedlings for all the expression profiling experiments performed here, the preparations contain a mixture of transcripts from all tissues. It seems plausible, therefore, that the transcripts that retain robust responsiveness to Rc in the *phyB* mutant

might be largely derived from the responsive apical-zone hook and cotyledon tissues. Because the cells in these tissues are, on average, smaller and more densely cytoplasmic than the hypocotyl cells (which are overall large and highly vacuolate), RNA from the apical-zone cells is likely to be strongly disproportionately represented in the preparations and, thus, dominate the microarray expression patterns. If this reasoning is correct, the 86% of genes that retain moderate to robust Rc responsiveness in the *phyB* mutant (Figure 6) are likely to have been derived primarily from apical-zone cells, where they are regulated largely by phyA, phyC, phyD, and/or phyE, and are not likely to be centrally involved in light-regulated hypocotyl cell expansion. Conversely, some or all the 14% of the genes that do display a significant degree of *phyB* regulation may be derived, at least partially, from hypocotyl cells, and be involved in their Rc-light-regulated expansion.

Extrapolation of this reasoning to the early-response, transcription-factor genes (Figure 7) suggests that one or more of the 11 such genes classified as significantly *phyB*-regulated in Rc, either early (*LHY*, *ZF3*, *ZF1*, *ZF6*, and *MYB-96*) or later (*CBF2*, *MYB-106*, *RAP2.6*, *ZF7*, *ATHB4*, and *bHLH-T61*) in the time-course, could be involved in regulating a branch of the transcriptional network that controls the process of hypocotyl cell elongation. On the other hand, any or all these genes might also be involved in mediating the partial regulation exerted by phyB on apical-zone tissues (Figures S1 and 8). The alternative that the Rc-induced changes in gene expression in the *phyB* mutant, detected over the first 24 h of irradiation, are not related to the phenotype often recorded after longer irradiation periods does not appear likely. This is because the visible phenotypic differences between WT and *phyB* are readily apparent within the first 12 h, and are well established within 24 h (R. Khanna, unpublished).

Conclusions: deciphering the phytochrome signaling and transcriptional network

Comparison of the expression patterns induced by FRc and Rc indicates a high degree of coincidence in the set of genes regulated by these two wavelengths of light during seedling de-etiolation. This is particularly so for the genes most robustly induced or repressed by the light signal, where the reliability of the measured change is highest. Although a range of apparent quantitative differences in the degree or pattern of responsiveness to FRc and Rc was observed, very few genes exhibited an absolute qualitative difference in wavelength responsiveness. The vast majority of genes displayed some degree of responsiveness to both wavelengths. Similarly, no markedly preferential regulation of any particular cellular process by either wavelength was apparent. We conclude, therefore, that the pathways transducing these two light signals converge early to regulate a largely common transcriptional network that functions to implement the seedling de-etiolation program. Strongly consistent with this conclusion, almost all the transcription-factor genes, identified as responding rapidly to FRc in our previous study (Tepperman *et al.*, 2001), are also early-response genes in Rc.

The data presented here indicate that, whereas phyB appears to be the dominant, if not exclusive, photoreceptor regulating suppression of hypocotyl cell expansion in response to Rc-light signals, this sensory function is shared, in apparently additive fashion, by one or more other phys in regulating other important aspects of the seedling de-etiolation process, namely, hook opening, cotyledon separation and expansion, and associated chloroplast biogenesis (Figure 8b). Thus, these data constitute evidence of organ-specific signaling activity among phy family members in response to Rc signals. This pattern is in striking contrast to the responsiveness of seedlings to FRc-light signals, where phyA is exclusively responsible for regulating all these facets of de-etiolation.

Transcript profiling indicates that the majority of Rc-responsive genes are not robustly regulated by phyB (Figure 6), and are therefore more likely to be involved in the processes driving apical-zone de-etiolation than controlling hypocotyl cell expansion. Conversely, the remaining minority of Rc-responsive genes display significant dependence on phyB to a greater or lesser extent (Figure 6), making some or all of them candidates for involvement in phyB-regulated hypocotyl cell elongation. However, because of the partial cotyledon phenotype in the *phyB* mutant (Figures S1 and 8a), it is not possible, from the present data, to unequivocally determine which, if any, of these genes is exclusively or selectively involved in hypocotyl responses. Nevertheless, the microarray data do identify an apparent bifurcation in the phy-regulated transcriptional network potentially responsible for organ-specific photomorphogenesis. This bifurcation appears unlikely to result from differential spatial expression patterns of the phys themselves, at least for phyA and phyB, as these are both apparently expressed ubiquitously in young seedlings (Somers and Quail, 1995a,b). In addition, it is clear that phyA is capable of acting in hypocotyl cells to suppress extension in response to FRc but not Rc signals (Figure S1). Thus, the selective activity of phyB in regulating hypocotyl cell expansion in response to Rc must arise by some other mechanism.

Examination of the genes that respond to the Rc signal within 1 h of exposure suggests that one or more of a subset of transcription-factor genes, classified as displaying the highest degree of phyB-dependence, may function in regulating the transcriptional activity of genes involved in hypocotyl cell expansion (Figure 7). Moreover, additional analysis focused on identifying genes that not only respond to Rc within 1 h, but also display robust differences

between WT and *phyB* within 1 h, provides evidence of a subset of these transcription-factor genes more likely to be direct targets of phyB signaling, including some that appear to be only transiently phyB-dependent (Figure 7, right-hand column). Other phyB-dependent, early-response genes that are intriguing in this respect are the signaling component-encoding genes, *EP1*, *SPA1*, and *GI*, and the hormone-regulated genes, auxin-induced protein (*AIP*)-*L*, *SAUR-AC-L*, *IAA20*, and *HOOKLESS1* (Table 3). These latter genes, together with *CELLULOSE SYNTHASE ISOLOG*, might be involved in early phyB-induced changes in hypocotyl, hook, and/or cotyledon cell expansion rates mediated by the auxin and ethylene systems. This general pattern is reinforced by the observation that several late-response genes, displaying relatively robust phyB-dependence, are also potentially involved in mediating regulation of cell expansion rates. These include *ARF-L*, *AUXIN-REGULATED GENE*, *ACC OXIDASE*, the GA-regulated gene, *GAST1*, and the potential cell growth-related genes *ENDOXYLOGLUCAN TRANSFERASE-LIKE* and *AQUAPORIN* (Table 3). Recently reported evidence that phyB in the cotyledons regulates auxin-responsive genes in the hypocotyl is also consistent with the above general pattern, and is suggestive of even greater complexity involving interorgan signaling (Tanaka *et al.*, 2002a,b).

More definitive determination of which phy family members (phyA, phyC, phyD, and/or phyE) are responsible for the residual Rc responsiveness in the *phyB* mutant will require analysis of higher-order phy mutants. Of particular interest will be the *phyA*/*phyB* double mutant, as there is evidence that this mutant has significantly reduced apical-zone Rc responsiveness compared to the phyB monogenic mutant (Franklin *et al.*, 2003; Reed *et al.*, 1993, 1994; R. Khanna, unpublished).

Experimental procedures

Plant growth and irradiation conditions

The *phyB1* mutant allele (Quail *et al.*, 1994) was introgressed into the ecotype RLD (T. Short, unpublished) and used throughout this study. WT RLD and *phyB* mutant seeds were sown on growth medium (GM) plates (Valvekens *et al.*, 1988) containing 0.9% agar, stratified for 5 days at 4°C, exposed to white light for 2 h to induce germination, and placed in a growth chamber at 21°C in total darkness for 4 days. Seedlings were then irradiated with Rc (660 nm, 7 μmol m^{-2} sec^{-1}), and tissue was harvested and frozen immediately in liquid nitrogen at 1-, 3-, 6-, 12-, 18-, and 24 h after the start of irradiation. Dark-control samples were harvested and frozen at 0 and 24 h. Triplicate, separately grown seedling batches were harvested at each of the time-zero, dark-control (D_0), and 1-h Rc-irradiation (R_1) time-points for both WT and *phyB* seedlings (six batches for the 1-h Rc-irradiated *phyB* samples) to provide biological replicates for independent RNA isolation and microarray hybridization for these samples. Single tissue samples were used at all other time-points.

RNA isolation, cRNA synthesis, and microarray hybridizations

Total RNA was prepared for each seedling batch separately (0.2 g tissue per batch) using the method of Chang *et al.* (1993), and processed for cRNA synthesis as previously described by Tepperman *et al.* (2001). High-density oligonucleotide arrays, containing probes of more than 8200 different *Arabidopsis* genes (Affymetrix, Santa Clara, CA, USA), were used for gene-expression detection as previously described by Tepperman *et al.* (2001).

Data analysis

The probe arrays were scanned with a Hewlett–Packard GeneArray Scanner, and expression levels for all gene sequences were determined using GENECHIP software, M.A.S. 5.0 (Affymetrix). The raw data were analyzed in Excel (Microsoft, Redmond, WA, USA). Data from a total of 27 separately prepared RNA samples that had each been hybridized separately to a different GENECHIP microarray were analyzed. These samples comprised: three time-zero dark-control samples (D_0) for WT; three D_0 samples for *phyB*; three 1-h Rc-irradiated (R_1) samples for WT; six R_1 samples for *phyB*; one sample each for 3-, 6-, 12-, 18-, and 24-h Rc-irradiated WT and *phyB*; and one sample each for 24-h dark-control (D_{24}) WT and *phyB*. Mean values were used for all data points for which we had triplicate microarrays. Values for all other time-points were from a single hybridization per treatment. To objectively define sequences exhibiting significant changes in abundance in response to Rc, we developed a set of quantitative criteria that were applied to each time-course data set. For each gene, the mean level of expression in the WT, dark-control seedlings at time zero was defined as the baseline to which all other signal values on the curve for that gene were compared. Initially, all genes displaying a twofold or greater deviation in expression from this reference value at one or more time-points on the curve for Rc-irradiated, WT seedlings were identified. The data for these genes were then subjected sequentially to a series of additional criteria designed to reduce the probability of inclusion of false-positives. Genes with no raw signal value greater than 25 were eliminated. Those with only one time-point greater than 25 were retained only if that value was for 24 h of Rc irradiation (R_{24}). Genes with only two data points greater than 25 were only retained if these data points were consecutive. Genes for which the dark-control 24-h (D_{24}) time-point was the maximum (induced genes) or minimum (repressed genes) value were eliminated. Only genes with a MFIR or a MFRR (WT/*phyB*) greater than 0.76 were included (see below). Finally, for all genes identified by these objective criteria, the full time-course curves were visually inspected individually for coherence and continuity. Genes displaying profiles that appeared to lack rational continuity or internal consistency, frequently because of apparent random fluctuations in signal intensity, especially with genes expressed at low levels, were eliminated (subjective de-selection). Data for these genes are accessible in Tables S28–S31.

For the 1-h Rc time-point, triplicate hybridization-intensity values for each of four the seedling samples (WT and *phyB* mutant, each at time zero (dark controls) and after 1 h of Rc irradiation) were analyzed. These values were obtained using at least three independent RNA samples (six in the case of the 1-h *phyB* mutant), separately prepared from three different tissue samples for each of the four treatments, each hybridized to a separate microarray chip (15 in total). The triplicate values for each gene were averaged and the SEs ($\pm$SE) were calculated. Genes for which the mean expression level in the Rc-irradiated WT at 1 h deviated twofold or more

from the mean time-zero, WT, dark-control level, and for which the SE bars for the Rc-irradiated WT did not overlap with those of the dark control were defined as 'early-response' genes. 'Late-response' genes were defined as those with at least one value (3–24 h) deviating twofold or more from the dark control at time zero.

For the present reanalysis of the previously described FRc experiment (Tepperman *et al.*, 2001), we used the same software and selection criteria as described above for the Rc experiment, with the additional criterion originally used, that at least one WT value between 1 and 24 h of FRc had to be twofold of that of the corresponding *phyA* mutant value at that time-point, in addition to being twofold the time-zero dark-control value.

To provide a quantitative estimate of the robustness of the responsiveness of each gene to the light treatment, we calculated a MFI value for induced genes, and a MFR value for repressed genes. MFI is defined as the sum of the expression values at each time-point from 1 to 24 h of exposure to light (L_1–L_{24}), divided by six times the WT time-zero dark-control (D_0) value.

$$\mathrm{MFI} = \frac{\mathrm{Sum}\ (L_1 - L_{24})}{(6 \times D_0\ (\mathrm{WT}))}$$

MFR is defined as the reciprocal of this function. Note that the WT D_0 value was used as the control value to calculate MFI and MFR values for both WT and mutant time-course curves. To compare the robustness of the responsiveness of each gene to the different wavelengths of light (FRc versus Rc) in the WT, or to different genotypes (WT versus mutant) in a single wavelength (Rc or FRc), we calculated a MFIR or MFRR value. For wavelength comparisons (e.g. FRc/Rc):

$$\mathrm{MFIR\ (or\ MFRR)} = \frac{\mathrm{MFI\ (or\ MFR)\ for\ WT\ in\ FRc}}{\mathrm{MFI\ (or\ MFR)\ for\ WT\ in\ Rc}}$$

For genotype comparisons (e.g. WT/*phyB* in Rc):

$$\mathrm{MFIR\ (or\ MFRR)} = \frac{\mathrm{MFI\ (or\ MFR)\ for\ WT\ in\ Rc}}{\mathrm{MFI\ (or\ MFR)\ for}\ \textit{phy B}\ \mathrm{in\ Rc}}$$

In order to avoid overestimates of MFI for induced genes, all WT D_0 values less than 10 were raised to a value of 10. Similarly, for repressed genes, all light values (L_1–L_{24}) less than 10 were raised to a value of 10.

Statistical analysis of fold-induction and -repression data

In order to calculate a statistical measure of significance for different MFI or MFR values between FRc and Rc wavelengths, or between the WT and *phyB* mutant, the individual fold-induction or -repression values at each time-point were calculated (the mean of the biological replicates was used to calculate values from the replicated time-points at 0 and 1 h). This gave a population of six individual fold-change values for each curve. A Student's *t*-test of the paired, one-tailed type was performed to test for a significant difference between the FRc and Rc wavelength means, and between the WT and *phyB* means (MFI or MFR). An appropriate null hypothesis was applied, for example, that the WT mean fold change was not greater than the mutant mean fold change for bins A–D, and that the mutant was not greater than the WT for bin E (Figures 4 and 5). To confirm significance independently of the assumption of normality inherent in the *t*-test, a *P*-value was also calculated using the Wilcoxon's Signed Rank test using the same null hypothesis. Both values are given in the supplemental data. All statistical calculations were performed using the programming language R (http://www.r-project.org/).

Acknowledgements

We thank Tim Short for the RLD line with the introgressed *phyB1* mutant allele, the members of our laboratory for stimulating discussions and comments on the manuscript, and Ron Wells for manuscript preparation. This work was supported by the Tory Mesa Research Institute, National Institutes of Health Grant 47475, Department of Energy grant DE-FG03-87ER13742, and Agricultural Research Service Grant 5335-21000-017-00D.

Supplementary Material

The following material is available from http://www.pgec.usda.gov/Quail/phyB.html

Figure S1. *phyA* and *phyB* null mutants display reciprocal photomorphogenic phenotypes in response to Rc or FRc.

Figure S2. Statistical evaluation of differential induction of gene expression by FRc and Rc in WT seedlings shown in Figure 2.

Figure S3. Statistical evaluation of differential repression of gene expression by FRc and Rc in WT seedlings shown in Figure 3.

Figure S4. Induced genes arrayed in rank order of relative responsiveness to FRc or Rc in WT *Arabidopsis* seedlings.

Figure S5. Repressed genes arrayed in rank order of relative responsiveness to FRc or Rc in WT *Arabidopsis* seedlings.

Figure S6. Early-response, transcription-factor genes displaying relatively robust differences in responsiveness to FRc and Rc in WT seedlings.

Figure S7. Early-response, transcription-factor genes displaying relatively small or no apparent differences of responsiveness to FRc and Rc in WT seedlings.

Figure S8. Late-response genes displaying relatively robust differences in responsiveness to FRc and Rc in WT seedlings.

Figure S9. Mean 24-h time-course expression profiles for all FRc- and Rc-responsive genes.

Figure S10. Statistical evaluation of differential induction of gene expression in WT and *phyB* seedlings in Rc shown in Figure 4.

Figure S11. Statistical evaluation of differential repression of gene expression in WT and *phyB* seedlings in Rc shown in Figure 5.

Figure S12. Early-response genes displaying relatively robust differences in responsiveness to Rc between WT and *phyB* null-mutant seedlings.

Figure S13. Late-response genes displaying relatively robust differences in responsiveness to Rc between WT and *phyB* null-mutant seedlings.

Figure S14. Genes displaying relatively small or no apparent differences in responsiveness to Rc between WT and *phyB* null-mutant seedlings.

Figure S15. Induced genes arrayed in rank order of relative responsiveness to Rc in WT compared to *phyB Arabidopsis* seedlings.

Figure S16. Repressed genes arrayed in rank order of relative responsiveness to Rc in WT compared to *phyB Arabidopsis* seedlings.

Figure S17. Temporal expression profiles for all early response transcription-factor genes identified as responding to FRc and/or Rc signals during seedling de-etiolation.

Figure S18. Induced genes arrayed in order of relative responsiveness to Rc at 1 h in WT compared to *phyB Arabidopsis* seedlings.

Figure S19. Repressed genes arrayed in order of relative responsiveness to Rc at 1 h in WT compared to *phyB Arabidopsis* seedlings.

Figure S20. Expression profiles after 1 h of irradiation for all early-response, transcription-factor genes identified as responding to FRc and/or Rc signals during seedling de-etiolation.

Note S1. Detailed description of the re-analysis of the FRc data from Tepperman *et al.* (2001) using M.A.S. 5.0.
Note S2. Apparent dichotomy in wavelength responsiveness is potentially misleading.
Note S3. Distribution of genes across wavelength-responsiveness bins.
Note S4. Distribution of functionally classifiable genes across wavelength-responsiveness bins and temporal-response categories.
Note S5. Analysis of early-response genes for the extent of phyB-contribution to the Rc response at 1 h.
Table S1 FRc master: data for FRc-irradiated WT and *phyA*; combined gene lists
Table S2 FRc induced: data for FRc-irradiated WT and *phyA*; FRc-induced genes only
Table S3 FRc repressed: data for FRc-irradiated WT and *phyA*; FRc-repressed genes only
Table S4 FRc early induced (1-h histograms): data for FRc-irradiated WT and *phyA*; early FRc-induced genes only
Table S5 FRc early repressed (1-h histograms): data for FRc-irradiated WT and *phyA*; early FRc-repressed genes only
Table S6 FRc early induced (time-course): data for FRc-irradiated WT and *phyA*; early FRc-induced genes only
Table S7 FRc early repressed (time-course): data for FRc-irradiated WT and *phyA*; early FRc-repressed genes only
Table S8 FRc late induced (time-course): data for FRc-irradiated WT and *phyA*; late FRc-induced genes only
Table S9 FRc late repressed (time-course): data for FRc-irradiated WT and *phyA*; late FRc-repressed genes only
Table S10 FRc 'non-responsive': data for FRc-irradiated WT and *phyA*; 'non-responsive' in FRc
Table S11 Rc master: data for Rc-irradiated WT and *phyB*; combined gene lists
Table S12 Rc induced: data for Rc-irradiated WT and *phyB*; Rc-induced genes only
Table S13 Rc repressed: data for Rc-irradiated WT and *phyB*; Rc-repressed genes only
Table S14 FRc_Rc WT master: data for FRc- and Rc-irradiated WT; combined gene lists
Table S15 FRc_Rc WT early induced (1-h histograms): data for FRc- and Rc-irradiated WT; early FRc- and Rc-induced genes
Table S16 FRc_Rc WT early repressed (1-h histograms): data for FRc- and Rc-irradiated WT; early FRc- and Rc-repressed genes
Table S17 FRc_Rc WT early induced (time-course): data for FRc- and Rc-irradiated WT; early FRc- and Rc-induced genes
Table S18 FRc_Rc WT early repressed (time-course): data for FRc- and Rc-irradiated WT; early FRc- and Rc-repressed genes
Table S19 FRc_Rc WT late induced (time-course): data for FRc- and Rc-irradiated WT; late FRc- and Rc-induced genes
Table S20 FRc_Rc WT late repressed (time-course): data for FRc- and Rc-irradiated WT; late FRc- and Rc-repressed genes
Table S21 Rc early induced (1-h histograms): data for Rc-irradiated WT and *phyB*; early Rc-induced genes only
Table S22 Rc early repressed (1-h histograms): data for Rc-irradiated WT and *phyB*; early Rc-repressed genes only
Table S23 Rc early induced (time-course): data for Rc-irradiated WT and *phyB*; early Rc-induced genes only
Table S24 Rc early repressed (time-course): data for Rc-irradiated WT and *phyB*; early Rc-repressed genes only
Table S25 Rc late induced (time-course): data for Rc-irradiated WT and *phyB*; late Rc-induced genes only
Table S26 Rc late repressed (time-course): data for Rc-irradiated WT and *phyB*; late Rc-repressed genes only
Table S27 Rc 'non-responsive': data for Rc-irradiated WT and *phyB*; 'non-responsive' in Rc
Table S28 Rc induced – duplicates: data for Rc-irradiated WT and *phyB*; Rc-induced duplicate probe sets and loci
Table S29 Rc repressed – duplicates: data for Rc-irradiated WT and *phyB*; Rc-repressed duplicate probe sets and loci
Table S30 Rc induced – deselected: data for Rc-irradiated WT and *phyB*; induced subjectively deselected genes
Table S31 Rc repressed – deselected: data for Rc-irradiated

References

Affymetrix (2001) *New Statistical Algorithms for Monitoring Gene Expression on GeneChip Probe Arrays.* Technical note no. 701097, Rev. 3.

von Arnim, A. and Deng, X.-W. (1996) Light control of seedling development. *Annu. Rev. Plant Physiol. Plant Mol. Biol.* **47**, 215–243.

Chang, S., Puryear, J. and Cairney, J. (1993) A simple and efficient method for isolating RNA from pine trees. *Plant Mol. Biol. Rep.* **11**, 113–116.

Devlin, P.F., Patel, S.R. and Whitelam, G.C. (1998) Phytochrome E influences internode elongation and flowering time in *Arabidopsis*. *Plant Cell*, **10**, 1479–1487.

Fankhauser, C. (2001) The phytochromes, a family of red/far-red absorbing photoreceptors. *J. Biol. Chem.* **276**, 11453–11456.

Fankhauser, C. and Chory, J. (1997) Light control of plant development. *Annu. Rev. Cell Dev. Biol.* **13**, 203–229.

Franklin, K.A., Praekelt, U., Stoddart, W.M., Billingham, O.E., Halliday, J. and Whitelam, G.C. (2003) Phytochromes B, D, and E act redundantly to control multiple physiological responses in *Arabidopsis*. *Plant Physiol.* **131**, 1–7.

Heim, M.A., Jakoby, M., Werber, M., Martin, C., Weisshaar, B. and Bailey, P.C. (2003) The basic helix-loop-helix transcription factor family in plants: a genome-wide study of protein structure and functional diversity. *Mol. Biol. Evol.* **20**, 735–747.

Hubbell, E., Liu, W.-M. and Mei, R. (2002) Robust estimators for expression analysis. *Bioinformatics*, **18**, 1585–1592.

Liu, W.-M., Mei, R., Di, X., Ryder, T.B., Hubbell, E., Dee, S., Webster, T.A., Harrington, C.A., Ho, M.-H., Baid, J. and Smeekens, S.P. (2002) Analysis of high density expression microarrays with signed-rank call algorithms. *Bioinformatics*, **18**, 1593–1599.

Ma, L., Li, J., Qu, L., Hager, J., Chen, Z., Zhao, H. and Deng, X.-W. (2001) Light control of *Arabidopsis* development entails coordinated regulation of genome expression and cellular pathways. *Plant Cell*, **13**, 2589–2607.

Neff, M.M., Fankhauser, C. and Chory, J. (2000) Light: an indicator of time and place. *Genes Dev.* **14**, 257–271.

Quail, P.H. (1998) The phytochrome family: dissection of functional roles and signaling pathways among family members. *Philos. Trans. R. Soc. Lond. B*, **353**, 1399–1403.

Quail, P.H. (2002a) Photosensory perception and signalling in plant cells: new paradigms? *Curr. Opin. Cell Biol.* **14**, 180–188.

Quail, P.H. (2002b) Phytochrome photosensory signalling networks. *Nat. Rev. Mol. Cell Biol.* **3**, 85–93.

Quail, P.H., Briggs, W.R., Chory, J. *et al.* (1994) Spotlight on phytochrome nomenclature. *Plant Cell*, **4**, 468–471.

Quail, P.H., Boylan, M.T., Parks, B.M., Short, T.W., Xu, Y. and Wagner, D. (1995) Phytochromes: photosensory perception and signal transduction. *Science*, **268**, 675–680.

Reed, J.W., Nagpal, P., Poole, D.S., Furuya, M. and Chory, J. (1993) Mutations in the gene for the red/far-red light receptor phytochrome B alter cell elongation and physiological responses throughout *Arabidopsis* development. *Plant Cell*, **5**, 147–157.

Reed, J.W., Nagatani, A., Elich, T.D., Fagan, M. and Chory, J. (1994) Phytochrome A and phytochrome B have overlapping but distinct functions in *Arabidopsis* development. *Plant Physiol.* **104**, 1139–1149.

Smith, H. (2000) Phytochromes and light signal perception by plants – and emerging synthesis. *Nature*, **407**, 585–591.

Somers, D.E. and Quail, P.H. (1995a) Phytochrome-mediated light regulation of *PHYA*- and *PHYB*-GUS transgenes in *Arabidopsis thaliana* seedlings. *Plant Physiol.* **107**, 523–534.

Somers, D.E. and Quail, P.H. (1995b) Temporal and spatial expression patterns of *PHYA* and *PHYB* genes in *Arabidopsis*. *Plant J.* **7**, 413–427.

Tanaka, S.-I., Nakamura, S., Mochizuki, N. and Nagatani, A. (2002a) Phytochrome in cotyledons regulates the expression of genes in the hypocotyl through auxin-dependent and -independent pathways. *Plant Cell Physiol.* **43**, 1171–1181.

Tanaka, S., Mochizuki, N. and Nagatani, A. (2002b) Expression of the *AtGH3a* gene, an *Arabidopsis* homologue of the soybean *GH3* gene, is regulated by phytochrome B. *Plant Cell Physiol.* **43**, 281–289.

Tepperman, J.M., Zhu, T., Chang, H.-S., Wang, X. and Quail, P.H. (2001) Multiple transcription-factor genes are early targets of phytochrome A signaling. *Proc. Natl. Acad. Sci. USA*, **98**, 9437–9442.

Toledo-Ortiz, G., Huq, E. and Quail, P.H. (2003) The *Arabidopsis* basic/helix-loop-helix transcription factor family. *Plant Cell*, **15**, 1749–1770.

Valvekens, D., Van Montagu, M. and van Lijsebettens, M. (1988) *Agrobacterium tumefaciens*-mediated transformation of *Arabidopsis thaliana* root explants by using kanamycin selection. *Proc. Natl. Acad. Sci. USA*, **85**, 5536–5540.

Whitelam, G.C. and Devlin, P.F. (1997) Roles of different phytochromes in *Arabidopsis* photomorphogenesis. *Plant Cell Environ.* **20**, 752–758.

Whitelam, G.C., Patel, S. and Devlin, P.F. (1998) Phytochromes and photomorphogenesis in *Arabidopsis*. *Philos. Trans. R. Soc. Lond. B Biol. Sci.* **353**, 1445–1453.

Yamashino, T., Matsushika, A., Fujimori, T., Sato, S., Kato, T., Tabata, S. and Mizuno, T. (2003) A link between circadian-controlled bHLH factors and the APRR1/TOC1 quintet in *Arabidopsis thaliana*. *Plant Cell Physiol.* **44**, 619–629.